

# 3D SPH Numerical Simulation of Dam Break Flow around Fixed Obstacles

Rezaldy Naufal Saleh, Dede Tarwidi\*, and Jondri

School of Computing, Telkom University

Jalan Telekomunikasi No. 1 Terusan Buah Batu, Bandung 40257, Indonesia

\*Corresponding author E-mail: [rezaldyns@icloud.com](mailto:rezaldyns@icloud.com)

## Abstract

Various efforts have been made to prevent coastal erosion. One of the efforts to prevent coastal erosion is to build breakwaters. This paper presents numerical modeling of fluid flow interaction with various shapes of breakwater. Fluid flow impact on different shapes of breakwater, i.e. trapezoidal prism, cylinder, and sphere has been investigated. The three-dimensional numerical modeling is purposed to decisive which breakwaters shape that can reduce the fluid velocity rapidly, compared to other tested breakwaters shapes. In this study, fluid motion is generated by dam break scheme. The fluid motion is governed by momentum and continuity equation. The equations of fluid motion are resolved by smoothed particle hydrodynamics (SPH) method. DualSPHysics, an open-source code based on SPH method, is applied to simulate fluid motion and the interaction with the blocks of breakwater. According to numerical results, the trapezoidal prism shape of breakwater can scale down the fluid velocity faster than the cylinder and sphere shape of breakwater with maximum velocity is about 2.20 m/s. Further, the cylinder shape yields the highest fluid velocity around the breakwater. The trapezoidal prism shape can be used as an effective breakwater

**Keywords:** SPH method, dam break, fixed obstacle, DualSPHysics, breakwater, numerical simulation

## 1. Introduction

Coastal erosion is not only caused by human factors but also by nature. Coastal erosion can be induced by tidal current, wave current, and wave action. Various efforts have been made to prevent coastal erosion. One of the efforts to prevent coastal erosion is building breakwaters. The structure of breakwater will affect the damage level of coastal erosion. The shape of breakwater highly influences to impact energy resulted. The effective shape of breakwater is the shape that will produce small impact energy. In other words, the breakwater should reduce the speed of the ocean wave when hitting the breakwater. In this case, it requires to design a breakwater that can reduce the speed of incident wave quickly.

To obtain an effective breakwater design, some researchers are more interested to conduct numerical simulations than conducting direct observations. Kawasaki (1999) investigated a numerical model for wave breaking due to a submerged breakwater and post-breaking wave deformation. His numerical results were verified by laboratory experimental data and it showed that the numerical model can produce well the wave deformation. Rogers, Dalrymple, & Stansby (2010) simulated the movement of caisson breakwater using 2-D SPH. Their numerical results for the displacement and the horizontal forces on the caisson showed promising agreement compared to experimental data. St-Germain et al. (2013) conducted numerical modelling of structures impacted by tsunami bores using SPH method. They compared the numerical results for water surface elevation with the experimental data. Moreover, Dentale et al. (2014) analyzed numerically the hydrodynamics aspects of the interactions between waves and emerged breakwaters. Their numerical results for run-up and reflection effect were compared with laboratory test.

One of the methods to simulate fluid flow and and the interaction with solid objects is smoothed particle hydrodynamics (SPH) method. DualSPHysics is open source code which is developed by SPH method. The code has been widely used in free-surface fluid simulation. Ni & Feng (2013) presented numerical simulation of wave run-up and overtopping on typical sloping dikes based on DualSPHysics. Their numerical results showed satisfactory agreements with experimental data. Altomare et al. (2014) used DualSPHysics code to simulate fluid-structure interaction for wave approaching a rubble mound breakwater. Their numerical results for run-up height were compared with experimental data and empirical solutions. They also showed that SPH method is suitable for practical applications in coastal engineering. Suzuki et al. (2015) explored applicability of DualSPHysics to derive drag coefficient in vegetation. Their numerical outputs showed good agreement compared to the values in other literatures. Moreover, Panalaran, Triatmadja, & Wygnyosukarto (2016) used DualSPHysics code to simulate wave forces on cylinders group. They concluded that the accuracy of numerical results were significantly influenced by particle size ratio of gap among cylinder piles.

In this work, fluid velocity around blocks of breakwater is studied. The fluid flow is induced by three-dimensional dam break. The motion of water is governed by Navier-Stokes and continuity equation. The smoothed particle hydrodynamics method is adopted to solve Navier-Stokes and continuity equation. The DualSPHysics is adopted to simulate fluid motion and its interaction with solid structures

(Crespo et al., 2015). Numerical modeling of various breakwaters, i.e. trapezoidal prism, cylinder, and sphere is conducted to obtain velocity behavior around the breakwaters.

## 2. Governing Equation

The motion of fluid is governed by momentum and continuity equation. The momentum equation which is also called the Navier-Stokes equation can be written as (Barreiro, 2016)

$$\frac{D\mathbf{v}}{Dt} = -\frac{1}{\rho}\nabla p + \mathbf{g} \quad (1)$$

where  $\mathbf{v}$ ,  $\rho$ ,  $p$ , and  $\mathbf{g}$  are vector velocity, density, pressure, and gravity per unit mass, respectively. Furthermore, the continuity equation can be expressed as

$$\frac{D\rho}{Dt} = -\rho\nabla \cdot \mathbf{v} \quad (2)$$

The fluid flow is considered as weakly compressible. Hence, the relationship between pressure and density of fluid is assumed to follow (Altomare et al., 2014)

$$p = B \left[ \left( \frac{\rho}{\rho_0} \right)^\gamma - 1 \right] \quad (3)$$

where  $B = c_0^2 \rho_0 / \gamma$ ,  $\gamma = 7$ ,  $\rho_0 = 1000 \text{ kg/m}^3$ , and  $c_0$  being the speed of sound at the reference density.

## 3. SPH Formulation

The SPH method is approached by an interpolation which consents a function to be formulated in terms of its value at number of points (Monaghan, 1992; Liu & Liu, 2003). Here, our goal is to discretize the governing equations (1) and (2) into number of particles using SPH method.

The first step of SPH method is by expressing arbitrary function  $f(\mathbf{x})$  into an integral form, i.e.

$$f(\mathbf{x}) = \int_{\Omega} f(\mathbf{x}') \delta(\mathbf{x} - \mathbf{x}') d\mathbf{x}' \quad (4)$$

where  $\Omega$  is the volume of the integral that contain  $\mathbf{x}$  and  $\delta(\mathbf{x} - \mathbf{x}')$  is the Diract delta function. The delta function can be replaced by smoothing function or kernel function,  $W$ . Hence, (4) becomes

$$\langle f(\mathbf{x}) \rangle = \int_{\Omega} f(\mathbf{x}') W(\mathbf{x} - \mathbf{x}', h) d\mathbf{x}' \quad (5)$$

Where  $h$  is smoothing length that represents influence area of kernel function. Moreover, the derivative of  $f(\mathbf{x})$  can be expressed as

$$\langle \nabla \cdot f(\mathbf{x}) \rangle = \int_{\Omega} f(\mathbf{x}') \cdot \nabla W(\mathbf{x} - \mathbf{x}', h) d\mathbf{x}' \quad (6)$$

By using (5) and (6), equation (1) can be expressed in the SPH form:

$$\frac{d\mathbf{v}_a}{dt} = -\sum_b m_b \left( \frac{p_b + p_a}{\rho_a \rho_b} \right) \nabla_a W(|\mathbf{r}_a - \mathbf{r}_b|, h) \quad (7)$$

Equation (7) represents discrete form of momentum equation with  $\mathbf{v}_a$ ,  $p_a$ , and  $\rho_a$  are velocity, pressure, density of particle a, respectively.  $m_b$  is mass of particle b which is neighbor particles of particle a. Moreover, the continuity equation (2) can be written in the SPH form as

$$\frac{d\rho_a}{dt} = \sum_b m_b (\mathbf{r}_a - \mathbf{r}_b) \cdot \nabla_a W(|\mathbf{r}_a - \mathbf{r}_b|, h) \quad (8)$$

Equation (7) and (8) are solved by using Verlet time stepping. The Quintic Wendland kernel is used as the kernel function  $W$ . For more comprehensive discussion about SPH method, the readers are suggested to review the literatures (Gingold & Monaghan 1977; Randles, 1996; Monaghan, 2005; Liu & Liu, 2010).

## 4. Results and Discussion

The numerical simulation is aimed to observe the effect of the breakwaters shape to fluid velocity when the fluid is approaching and hitting the breakwaters. In this study, there are three different shapes of breakwaters that are trapezoidal prism, cylinder, and sphere. The simulation uses DualSPHysics code (Altomare et al., 2014) which has been widely used to simulate fluid problems. DualSPHysics is a software-based SPH method that can run on the CPU or GPU. In this simulation, the three scenarios are running on the GPU with computer specification as follows. GPU: GeForce GTX 950, CPU: Intel® Core™ i3-2120 CPU@3.3GHz, and Memory: 4.00 GB RAM. The open-source Paraview software (Ahrens, Geveci, & Law, 2005) is used to visualize fluid flow around breakwaters. We also show more realistic visualization by using open-source Blender software.

Fig. 1 shows initial setup of dam break simulation with dam size is  $0.39 \text{ m} \times 0.66 \text{ m} \times 0.29 \text{ m}$ . In this simulation, 128309 SPH particles are used to simulate fluid motion. Points  $(0.754, 0.31, 0.02)$ ,  $(0.754, 0.31, 0.04)$ , and  $(0.754, 0.31, 0.06)$  are observation points which is used to measure fluid velocity breakwaters. The trapezoidal prism breakwater has height of 0.3 m and bottom and top area of  $0.019 \text{ m}^2$  and  $0.0038 \text{ m}^2$  respectively. Furthermore, the cylinder shape has diameter of 0.09 m and height of 0.19 m while the sphere shape has diameter of 0.14 m. The simulation is started when one of the dam wall is broken out and then the fluid hits the breakwaters.

Fluid flow around trapezoidal prism, cylinder, and sphere breakwaters for  $t = 0.4 \text{ s}$ ,  $t = 0.6 \text{ s}$ ,  $t = 0.8 \text{ s}$ , and  $t = 1.0 \text{ s}$  is shown by Fig. 2, Fig. 3, and Fig. 4 respectively. From these figures, it can be observed that each breakwater has different form of fluid flow. For instance, at  $t = 0.4 \text{ s}$ , there is more fluid flowing upward after hitting the trapezoidal prism shape compared to cylinder and sphere shapes. At  $t = 0.6 \text{ s}$ , there is no fluid through the holes between trapezoidal prism breakwaters. It can be observed that trapezoidal prism breakwaters is more effective to scale down the fluid velocity than other breakwaters.

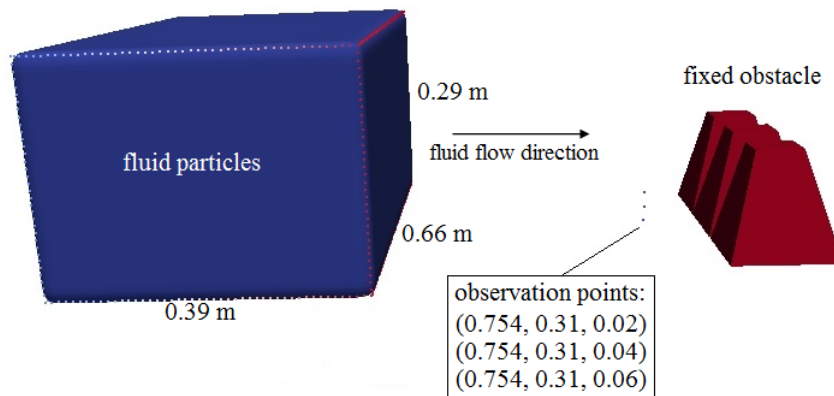


**Fig. 1:** Initial setup of dam break simulation with 128309 SPH fluid particles.

We also develop more realistic visualization of fluid flow around breakwaters. Here, we use Blender, a powerful 3D visualization software for fluid flow. Fig. 5 depicts 3D fluid flow around trapezoidal prism, cylinder, and sphere breakwaters which is rendered by Blender. As can be seen from the figure, the motion of water and how it behaves when hitting the breakwaters have approached the real water motion. However, the accuracy of this simulation can only be obtained by comparing it with experimental results.

Fluid velocity comparison of various breakwaters at point  $(0.754, 0.31, 0.02)$  is shown by Fig. 6. From the figure, it can be observed that each breakwater produces maximum velocity of fluid in x axis direction is almost similar, i.e. approximately 2.49 m/s. Here, trapezoidal prism can decrease the fluid velocity rapidly than other shapes meanwhile the cylinder yields higher fluid velocity before and after the fluid hitting the breakwater compared to other breakwaters. Moreover, at  $t = 1.0 \text{ s}$ , the fluid that flows trapezoidal prism has velocity of 0.014 m/s while the cylindrical and sphere breakwaters still have velocity of 0.354 m/s and 0.109 m/s respectively.

Fig. 7 depicts the fluid velocity at point  $(0.754, 0.31, 0.04)$  when hitting trapezoidal prism, cylinder, and sphere breakwaters. At this point, the maximum velocity of fluid is about 2.46 m/s which is smaller than fluid velocity at point  $(0.754, 0.31, 0.02)$ . Furthermore, at  $t = 1.0 \text{ s}$ , the trapezoidal prism, cylinder, and sphere breakwaters have velocity of  $-0.001 \text{ m/s}$ ,  $0.308 \text{ m/s}$ , and  $0.089 \text{ m/s}$  respectively. The negative velocity means that the direction of fluid has changed with the reverse direction since the fluid hitting the breakwater. It can also be seen that, at this point of observation, the trapezoidal prism can decrease the fluid velocity quickly compared to other breakwaters.

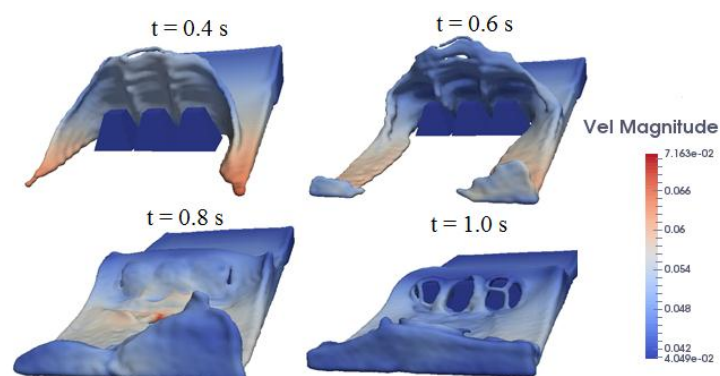


**Fig. 2:** Simulation result for trapezoidal prism obstacle at  $t = 0.4 \text{ s}$ ,  $t = 0.6 \text{ s}$ ,  $t = 0.8 \text{ s}$ , and  $t = 1.0 \text{ s}$ .

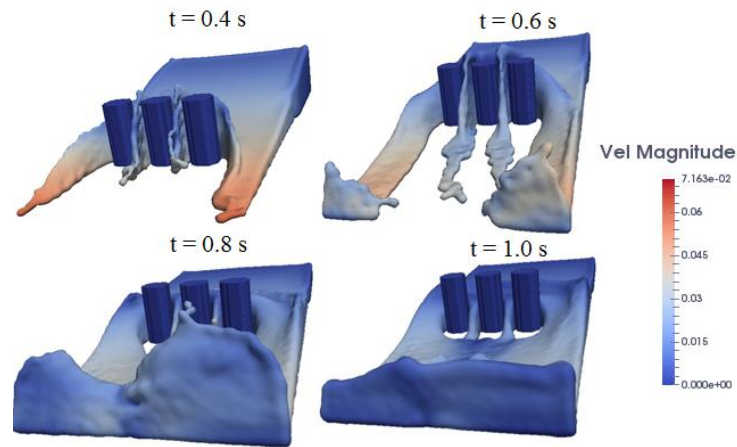


**Fig. 3:** Simulation results for cylinder obstacle at  $t = 0.4$  s,  $t = 0.6$  s,  $t = 0.8$  s, and  $t = 1.0$  s.

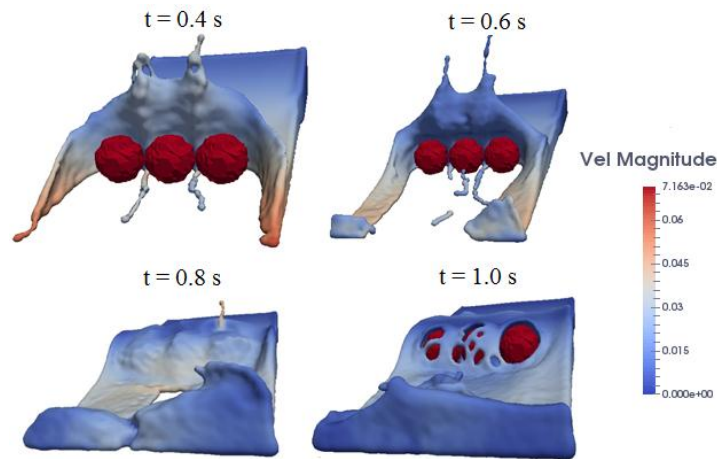


**Fig. 4:** Simulation results for sphere obstacle at  $t = 0.4$  s,  $t = 0.6$  s,  $t = 0.8$  s, and  $t = 1.0$  s.

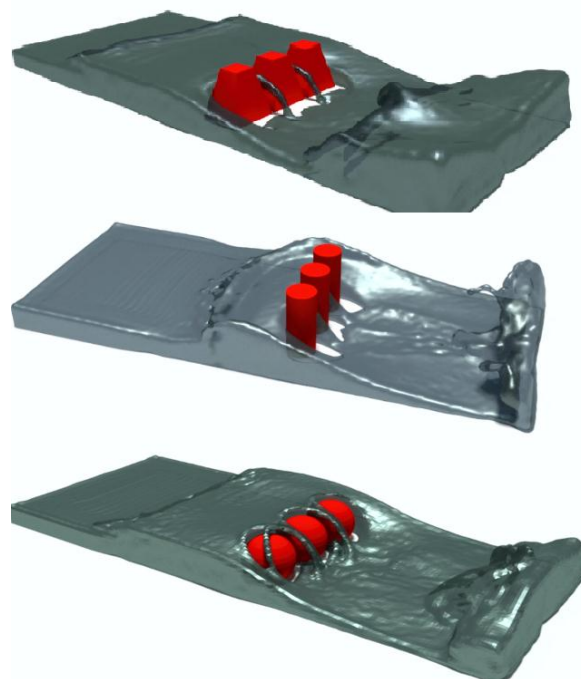


**Fig. 5:** Blender visualization for trapezoidal prism obstacle (top image), cylinder obstacle (middle image), and sphere obstacle (bottom image).

The fluid velocity at point (0.754, 0.31, 0.06) in x direction for trapezoidal prism, cylinder, and sphere obstacles is displayed by Fig. 8. The maximum velocity of fluid is 2.20 m/s, 2.31 m/s, and 2.26 m/s for trapezoidal prism, cylinder, and sphere obstacles, respectively. It can be observed that, at this point, it has different maximum velocity for different obstacle with trapezoidal prism is the smallest. At  $t = 1.0$  s, the fluid velocity for trapezoidal prism, cylinder, and sphere obstacles is 0.006 m/s, 0.172 m/s, and 0.071 m/s.

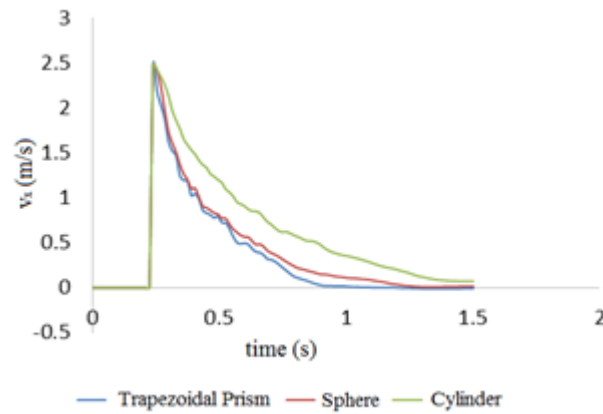


Fig. 6: Velocity in x axis direction ( $v_x$ ) at point (0.754, 0.31, 0.02) for the various obstacles.

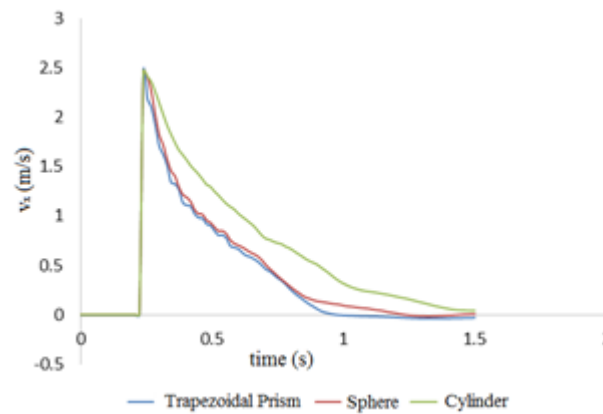


Fig. 7: Velocity in x axis direction ( $v_x$ ) at point (0.754, 0.31, 0.04) for the various obstacles.

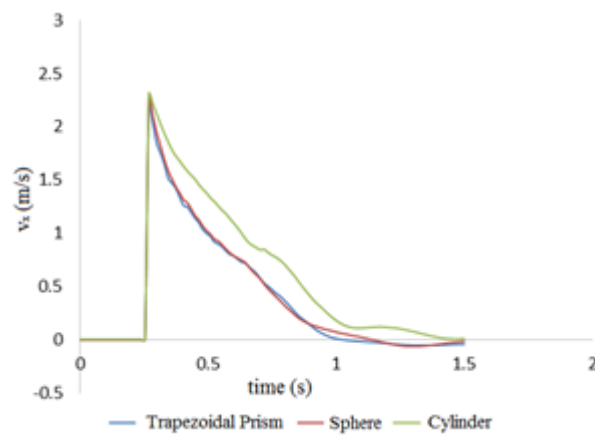


Fig. 8: Velocity in x axis direction ( $v_x$ ) at point (0.754, 0.31, 0.06) for the various breakwaters.

As can be seen from the figures, we can observe that the trapezoidal prism breakwater can scale down the fluid velocity rapidly compared to other breakwaters with the maximum velocity is about 2.20 m/s. From the numerical results, it can be obtained that the higher fluid particles position around breakwaters the lower fluid velocity resulted. Moreover, the cylinder breakwater can produce the highest velocity of fluid when hitting and passing the breakwater.

## 5. Conclusion

Numerical modeling of fluid flow interaction with various shapes of breakwater i.e. trapezoidal prism, cylinder, and sphere has been successfully conducted. According to the numerical simulation, the trapezoidal prism shape of breakwater can scale down the fluid velocity rapidly compared to other shape of breakwater with maximum velocity is about 2.20 m/s. Further, the cylinder shape yields the highest fluid velocity around the breakwater. The trapezoidal prism geometry can be applied as an effective breakwater.

## References

- [1] Ahrens, J., Geveci, B., & Law, C. (2005). 36-ParaView: An End-User Tool for Large-Data Visualization. *Visualization Handbook*, 717-731.
- [2] Barreiro, A., Crespo, A. J. C., Dominguez, J. M., Garcia-Feal, O., Zabala, I., & Gomez-Gesteira, M. (2016). Quasi-static mooring solver implemented in SPH. *Journal of Ocean Engineering and Marine Energy*, 2(3), 381-396.

- [3] Altomare, C., Crespo, A. J., Rogers, B. D., Domínguez, J. M., Gironella, X., & Gómez-Gesteira, M. (2014). Numerical modelling of armour block sea breakwater with smoothed particle hydrodynamics. *Computers & Structures*, 130, 34-45.
- [4] Crespo, A. J., Domínguez, J. M., Rogers, B. D., Gómez-Gesteira, M., Longshaw, S., Canelas, R., ... & García-Feal, O. (2015). DualSPHysics: Open-source parallel CFD solver based on Smoothed Particle Hydrodynamics (SPH). *Computer Physics Communications*, 187, 204-216.
- [5] Dentale, F., Donnarumma, G., & Carratelli, E. P. (2014). Simulation of flow within armour blocks in a breakwater. *Journal of coastal research*, 30(3), 528-536.
- [6] Gingold, R. A., & Monaghan, J. J. (1977). Smoothed particle hydrodynamics: theory and application to non-spherical stars. *Monthly notices of the royal astronomical society*, 181(3), 375-389.
- [7] Kawasaki, K. (1999). Numerical simulation of breaking and post-breaking wave deformation process around a submerged breakwater. *Coastal Engineering Journal*, 41(3&4), 201-223.
- [8] Liu, G. R., & Liu, M. B. (2003). *Smoothed particle hydrodynamics: a meshfree particle method*. World Scientific.
- [9] Liu, M. B., & Liu, G. R. (2010). Smoothed particle hydrodynamics (SPH): an overview and recent developments. *Archives of computational methods in engineering*, 17(1), 25-76.
- [10] Monaghan, J. J. (1992). Smoothed particle hydrodynamics. *Annual review of astronomy and astrophysics*, 30, 543-574.
- [11] Monaghan, J. J. (2005). Smoothed particle hydrodynamics. *Reports on progress in physics*, 68(8), 1703.
- [12] Ni, X. Y., & Feng, W. B. (2013). Numerical simulation of wave overtopping based on DualSPHysics. In *Applied Mechanics and Materials* (Vol. 405, pp. 1463-1471). Trans Tech Publications.
- [13] Panalaran, S., Triatmadja, R., & Wignyosukarto, B. S. (2016, July). Mathematical modelling of wave forces on cylinders group using DualSPHysics. In *Advances of Science and Technology for Society: Proceedings of the 1st International Conference on Science and Technology 2015 (ICST-2015)* (Vol. 1755, No. 1, p. 060004). AIP Publishing.
- [14] Randles, P. W., & Libersky, L. D. (1996). Smoothed particle hydrodynamics: some recent improvements and applications. *Computer methods in applied mechanics and engineering*, 139(1), 375-408.
- [15] Rogers, B. D., Dalrymple, R. A., & Stansby, P. K. (2010). Simulation of caisson breakwater movement using 2-D SPH. *Journal of Hydraulic Research*, 48(S1), 135-141.
- [16] St-Germain, P., Nistor, I., Townsend, R., & Shibayama, T. (2013). Smoothed-particle hydrodynamics numerical modeling of structures impacted by tsunami bores. *Journal of Waterway, Port, Coastal, and Ocean Engineering*, 140(1), 66-81.
- [17] Suzuki, T., Oyaizu, H., Altomare, C., Crespo, A. J., & Domínguez, J. M. (2015). Applicability of DualSPHysics model to derivation of drag coefficient in vegetation. In *36th IAHR World Congress* (pp. 1-7).
- [18] Tarwidi, D. (2016). Smoothed Particle Hydrodynamics Method for Two-dimensional Stefan Problem. *arXiv preprint arXiv:1602.06672*.